0 0 0 0 4 2 0 , 9 3 4

Submitted to Journal of Materials Science

LBL-3189
Preprint c.1

LAWRENCE
RADIATION LABORATORY

LIBRARY AND
DOCUMENTS SECTION

DIRECT OBSERVATION OF LIQUID-PHASE SINTERING IN THE SYSTEM TUNGSTEN CARBIDE-COBALT

Leonard Froschauer and Richard M. Fulrath

October 1974

Prepared for the U. S. Atomic Energy Commission
under Contract W-7405-ENG-48

For Reference

Not to be taken from this room

LAWRENCE BERKELEY LABORATORY
UNIVERSITY OF CALIFORNIA
BERKELEY

LBL-3189
c.1

DISCLAIMER

This document was prepared as an account of work sponsored by the United States Government. While this document is believed to contain correct information, neither the United States Government nor any agency thereof, nor the Regents of the University of California, nor any of their employees, makes any warranty, express or implied, or assumes any legal responsibility for the accuracy, completeness, or usefulness of any information, apparatus, product, or process disclosed, or represents that its use would not infringe privately owned rights. Reference herein to any specific commercial product, process, or service by its trade name, trademark, manufacturer, or otherwise, does not necessarily constitute or imply its endorsement, recommendation, or favoring by the United States Government or any agency thereof, or the Regents of the University of California. The views and opinions of authors expressed herein do not necessarily state or reflect those of the United States Government or any agency thereof or the Regents of the University of California.

0 0 0 0 4 2 0 1 9 5 5

DIRECT OBSERVATION OF LIQUID-PHASE SINTERING IN THE SYSTEM TUNGSTEN CARBIDE-COBALT

Leonard Froschauer and Richard M. Fulrath

Inorganic Materials Research Division, Lawrence Berkeley Laboratory
and Department of Materials Science and Engineering,
College of Engineering; University of California,
Berkeley, California 94720

Synopsis

The hot-stage of a scanning electron microscope has been used to observe liquid-phase sintering in the system tungsten carbide-cobalt. Densification behavior and the mechanism for the first, fast stage of sintering have been determined; the influence of particle size and the amount of liquid phase has been investigated. In all samples the densification kinetics is that of a rearrangement process; direct observation confirmed this result.

1. Introduction

Liquid-phase sintering is an important fabrication process. It is necessary that the relation between the properties of a system and the developing density and microstructure be understood. The availability of a hot stage for the scanning electron microscope with the necessary temperature capability [1] allowed a new approach to the study of densification in many systems. A discussion of the advantages and problems encountered in this technique can be found in [2].

WC-Co is an interesting system for an examination of liquid phase sintering from two different points of view: it is a material of great practical importance and it is theoretically interesting because it is one of the systems where complete densification is reached in very short times. This is due to the properties of the system that are essential

for good sintering behavior: complete wetting, zero dihedral angle, and solubility of WC in the liquid metal phase. For a discussion of the proposed densification mechanisms in liquid phase sintering and of the possible influences of the properties of the system on the densification, see [3].

The fast densification (rearrangement) after the first appearance of the liquid phase in this system is an obstacle for a determination of sintering kinetics. The very few shrinkage measurements for the early stage, using direct optical observation of the sample, by KINGERY et al. [4], CECH [5], and EXNER [6] find a time-proportional shrinkage that leads to nearly theoretical density within 2 min of sintering for samples with more than 7 wt% cobalt and tungsten carbide particle sizes of less than 3 μm. For lower amounts of liquid phase or for coarser particles, a second, slower densification region follows. KINGERY [4] found for this part of the densification curve a time exponent of 1/3. These observed kinetics correspond with KINGERY's model calculations [7] for rearrangement and diffusion-controlled solution-precipitation. These mechanisms have been accepted.

There are, however, problems in this interpretation. EXNER [6] also measured linear shrinkage for WC-10 wt% Co sintered below the eutectic temperature. He found an activation energy for densification in this stage of 60 kcal/mol. This same activation energy was also determined above the melting point. This seems to suggest that the presence of the liquid phase has no influence on sintering and so EXNER doubts the validity of KINGERY's model without proposing another mechanism.

For the second densification stage (solution-precipitation), a slope of 1/3 in the $\Delta L/Lo$ vs ln time plot is subject to question. PRILL et al. [8] and EXNER [6] argue that a solution-precipitation process starts only after the rearrangement has ceased so that the time zero and initial density have to be chosen at the end of stage I. A replot of KINGERY's data under this assumption changes the slope significantly. This replot seems to be very sensitive to the choice of time zero, because the two authors get different results for the same curve reported by KINGERY (1.0 [6]) and .5 [8]).

A third point is that KINGERY's method of separating the densification curve into at least two parts with constant time exponents does not seem to be necessary. Shrinkage measurements for these curves show a continuous change of slope [3,6].

This work was undertaken to apply the new technique of hot-stage scanning electron microscopy in order to get a continuous determination of shrinkage and a parallel observation of microstructure. This should be especially helpful to obtain new results for the first, fast part of the densification.

2. Experimental Procedure

The starting powders were commercial tungsten carbide and cobalt, sieved into different size fractions. The WC particle size fractions were <10 μm (Fischer SSS 2.2 μm), 10-20 μm, and 20-30 μm, the cobalt was always in the same size range. Mixtures of the two powders with 2, 4, 6, and 10 wt% cobalt were prepared by mixing in alcohol for 24 h. Samples 3/16 in. diameter were cold-pressed to green densities of about 60% theoretical density. In addition, commercial samples with the same

Co contents have been used. The WC-10 wt% Co was provided by Plansee Werke, Austria; the particle size of the WC before 120 h of milling was reported as 2.5 μm. The samples with 2, 4, and 6 wt% Co were provided by Friedr. Krupp GmbH, Germany; the WC particle size of this material was .8 μm.

To remove oxide films from the surfaces, all samples were prefired for one h at 800°C in helium-4% hydrogen. The sintering was carried out in the hot-stage of a scanning microscope; the details have been described previously [2]. For controlled heating experiments, the samples were heated to 1150°C in about 5 min, held isothermally for another 5 min and then heated to 1380°C at a constant rate. In an experiment to determine isothermal sintering, the samples were heated from 1000°C to about 1380°C in about .8 min and held at this temperature.

3. Results and Discussion

3.1. Influence of liquid-phase volume on shrinkage

To find the influence of different parameters (content of liquid phase, particle size, temperature), a series of experiments was performed. Figs. 1 and 2 show densification curves for the commercial samples WC-Co 2 to WC-Co 10 for a heating rate of 4°C/min and the very fast heating.

From the experiments with controlled heating rate (fig. 1) it is observed that below the eutectic temperature of about 1320°C the shrinkage is not very sensitive to the amount of cobalt. Assuming that for the low densities in this region during the heating the densification rate is independent of density, we can calculate the densification rate $d(\Delta L/L_o)/dt$ and plot its logarithm as a function of 1/T. Below the

eutectic temperature this plot results in a linear function with an activation energy of about 80 kcal/mol. This result is in reasonable agreement with EXNER's result of 60 kcal/mol, but the absolute value of the densification rate was much higher in EXNER's experiments.

At the eutectic temperature the different samples show different behavior. The specimens with 10% Co (i.e. about 22 vol% liquid phase at 1350°C) show a marked increase in densification rate and reach nearly theoretical density within minutes. This change in densification rate at the melting point is different to EXNER's result of a constant activation energy above and below the eutectic temperature. The plot log (densification rate) vs 1/T results in a marked increase in the densification rate compared to the solid state sintering. The curve cannot be respresented by a straight line and an activation energy cannot be determined. The specimens with 2% cobalt (roughly 5 vol% liquid phase) show hardly any influence of the formation of liquid phase.

Fig. 2 shows the densification for the fast heating experiments. Starting at time zero the sample cup was heated from 1000°C to about 1380°C within .8 min; the shrinkage results suggest that the samples reach the melting point with a delay of about .1 to .2 minutes. After melting, all specimens show fast shrinkage. The relative volume change in this stage is nearly proportional to the amount of liquid phase.

To find the time-exponents of the densification, the logarithm of linear shrinkage for the fast heated samples has been plotted vs. log time (fig. 3). At time zero the time of the sharp increase in density from fig. 2 has been chosen. The curve for WC-Co 10 is nearly identical with the results of EXNER for a similar material. The first part of the

densification curves can be well represented by a time-exponent of 1 in agreement with the linear shrinkage reported in the literature and with KINGERY's model for rearrangement. The linear densification rate ($\Delta L/L_o$/min) depends slightly on the amount of liquid phase (.23/min for WC-Co 2, .35/min for WC-Co 6). The slower densification for WC-Co 10 is due to the larger particle size.

The second part of the densification curves has a slope of about .2. Replotting the data after subtracting the contribution of the first part changes this slope to .5 in good agreement with the results of PRILL [8].

3.2. Influence of particle size on shrinkage

In figs. 4 to 6 the density for WC-Co 10 with different particle sizes has been plotted for two different heating rates and the fast heating experiments. The fastest densification has always been recorded in the commercial samples (with a particle size of 2.5 μm before 120 h of milling), the densification decreases with increasing particle size.

The samples with the larger particles show hardly any densification in the solid state. At the eutectic point, in all samples a region of fast densification is found. The kinetics in this region can be represented by a linear relation between shrinkage and time. The densification rate decreases slightly with increasing particle size, but it is very difficult to establish a function for this parameter from the available data. To find an actual particle size dependence of the densification rate, a series of experiments with narrow size fractions of particles would be necessary.

The important result of these experiments is that for a constant amount of liquid phase the shrinkage during this linear stage is very

dependent on particle size. Densification curves for WC-Co 4 and WC-Co 10 of two particle sizes (fig. 7) show that this particle size influence is very strong and that the fine material with about 9% liquid phase densifies faster than a coarse material with 22% liquid phase. It is quite difficult to find a quantitative relationship from the available data, but it can be proposed from these results that for WC-Co 10 the exponent in a relation $\Delta L/L_o = k.d^{-n}$ for stage I is between .5 and 1.

3.3. Densification mechanism

The shrinkage measurements lead to the conclusion that the mechanism for the first densification after melting is a rearrangement process. For this mechanism the determined kinetics are in agreement with KINGERY's model calculations. The influence of the amount of liquid phase and the particle size on the densification rate and overall densification can be qualitatively rationalized.

It is known from earlier investigations that the densification kinetics do not necessarily allow one to make conclusions on the actual mechanism. In the system Fe-Cu it has been shown that in spite of a time-proportional shrinkage densification does not occur by a rearrangement process [3].

In the system WC-Co, however, direct observation of the melting process and the subsequent sintering confirms the presence of a rearrangement stage. The available magnification of the SEM with the hot stage did not allow the resolution of the small particle sizes, but the rearrangement process can be observed in the samples with 10 to 20 μm particles. It is reasonable to assume that the process is even more probable for smaller particles.

Figs. 8 and 9 show samples WC-Co 10 and Wc-Co 15 (10-20 μm) during sintering. In fig. 8 CRT pictures from the SEM are displayed; the pictures of fig. 9 are single frames from a continuous movie film taken from the TV screen of the SEM with a framing speed of 2 frames/sec. It can be seen in these figures, and even better in a continuous film, that for a short time at and after melting, a strong movement of the particles relative to their neighbors occurs. This movement leads to a more effective packing and thus to an overall densification. The degree of rearrangement on a quantitative basis has not been made, but it can be observed that this rearrangement process is responsible for the densification during the period immediately after melting.

The properties of this system make rearrangement possible. In a completely wetting system, only interfaces solid-solid, solid-liquid, and liquid-vapor should be present; the energy of the liquid-vapor interface (the surfaces of the pores) is for the driving force for sintering. The capillary pressure of the pores acts like a hydrostatic pressure on the whole system. This pressure leads to a viscous flow and to shrinkage, if one of two conditions are fulfilled: either the diffusion in the solid phase is so low that no necks between adjacent solid particles are formed during the heating, or the dihedral angle is zero and after melting, the liquid phase penetrates into the necks and solid-solid interfaces are eliminated. It is reasonable to assume that in addition to the zero-dihedral angle some solubility of the solid in the liquid phase is necessary in order to dissolve the material at the points of contact. Either of these conditions helps to avoid the formation of a rigid skeleton of the solid particles that is not able to rearrange.

WC-Co fulfills all of these requirements. The melting point of WC is relatively high (T_m(eutectic)/T_m(WC) = .6), so that below the melting point little diffusion is possible, the dihedral angle is probably 0° (see discussion in [9]) and there is solubility of WC in the liquid phase.

The densification results described in 3.1 and 3.2 can be understood for a rearrangement process. As described, the system behaves as if under hydrostatic compression due to the capillary pressures of pores. The influence of different parameters should be similar to the results found for the behavior of suspensions under stress. Unfortunately, there are no exact theories for suspensions with high amounts of solid phase. The presence of pores is another complication, but a qualitative explanation for many phenomena can be found.

The viscosity of a suspension increases with the amount of solid phase [10]. This means for our system the densification rate for a constant driving force (i.e. constant pore size) decreases with decreasing amount of liquid phase.

The decreasing amount of densification with decreasing amounts of liquid phase has been predicted by KINGERY, he assumed a linear relationship. The described model would explain this result as follows: the viscosity increases not only with increasing amounts of solid phase, but also with decreasing porosity. Therefore, the deformability of the system decreases with increasing density. There is a point where the nearly constant compression force does not result in a measurable viscous flow; the rearrangement stops. Because the compressive force depends only slightly on the amount of liquid phase, the samples with low amounts

of liquid, i.e. higher viscosity, reach this point at lower density.

The effect of particle size can be explained by a change in driving force. The pore size in the composite is roughly equal to the particle size; with increasing particle size the pore size increases and because of the capillary force of a pore being proportional 1/r, the compressive pressure on the system decreases. This decrease in driving force is apparently stronger than the increasing deformability with increasing particle size found for suspensions [11].

4. Conclusions

Direct observation of liquid phase sintering in the hot stage of a scanning electron microscope could prove that the first, fast densification observed in WC-Co at the melting point of the eutectic phase is connected with a rearrangement process. This confirms that this mechanism postulated earler is actually occurring. The microstructural parameters (liquid volume and solid particle size) effect on densification rate and shrinkage in this stage agree with the rearrangement process.

Acknowledgments

This work was supported by the United States Atomic Energy Commission through the Inorganic Materials Research Division of the Lawrence Berkeley Laboratory and by the Deutsche Forschungsgemeinschaft.

References

1. R. M. FULRATH, 5th Annual Scanning Electron Microscopy Symposium, Chicago, 1972.

2. R. M. FULRATH, L. FROSCHAUER and D. N. K. WANG, submitted for publication to J. of Microscopy.

3. L. FROSCHAUER and R. M. FULRATH, submitted for publication to J. of Mat. Sci.

4. W. D. KINGERY, E. NIKI, and M. D. NARASIMHAN, J.Am. Ceram. Soc., 44 (1961) 29-35.

5. B. CECH, Sov. Powder Met. (1963) 86-92.

6. H. E. EXNER, Internat. Pulvermet. Tagung, Bad Eisenach (1965).

7. W. D. KINGERY, J. Appl. Phys. 30 (1959) 301-306.

8. A. L. PRILL, H. W. HAYDEN, and J. H. BROPHY, Trans. AIME, 233 (1965) 960-965.

9. T. J. WHALEN and M. HUMENIK in Sintering and Related Phenomena, ed. G. KUCZYNSKI, pp. 715-746 (1965).

10. L. HOLLIDAY, Composite Materials, Elsevier (1966).

11. L. FROSCHAUER, Ph.D. Thesis, Erlangen (1972).

Figure Captions

Fig. 1. Densification of commercial WC-Co mixtures as a function of temperature and time at 1380°C when heated at 4°C/min to 1380°C.

Fig. 2. Densification of commercial WC-Co mixtures as a function of time when rapidly heated from 1000°C to 1350°C in approximately .8 min. Time zero is taken at the start of rapid heating.

Fig. 3. Log of linear shrinkage vs log time for the data given in fig. 2 for commercial WC-Co mixtures.

Fig. 4. Densification of WC-10 wt% Co compacts heated at 11°C/min to 1380°C then held isothermally. Particle size is for WC particles in the green compact.

Fig. 5. Densification of WC-10 wt% Co compacts heated at 4°C/min to 1380°C then held isothermally.

Fig. 6. Densification of WC-10 wt% Co compacts as a function of time when rapidly heated from 1000°C to 1350°C in approximately .8 min. Time zero is taken at the start of rapid heating.

Fig. 7. Densification of WC-Co compacts heated at 4°C/min to 1380°C then held isothermally.

Fig. 8. Photographs of a WC-10 Co compact taken at the indicated temperatures while heating at a constant rate to 1415°C. The WC particles are between 10 to 20 μm in size.

Fig. 9. Photographs taken from the SEM television monitor during continuous filming of the liquid phase formation in a WC-Co 15 compact. The liquid phase formed between the top left and top right photographs. The WC particles are 10 to 20 μm in diameter.

0 0 0 0 4 2 0 1 9 6 1

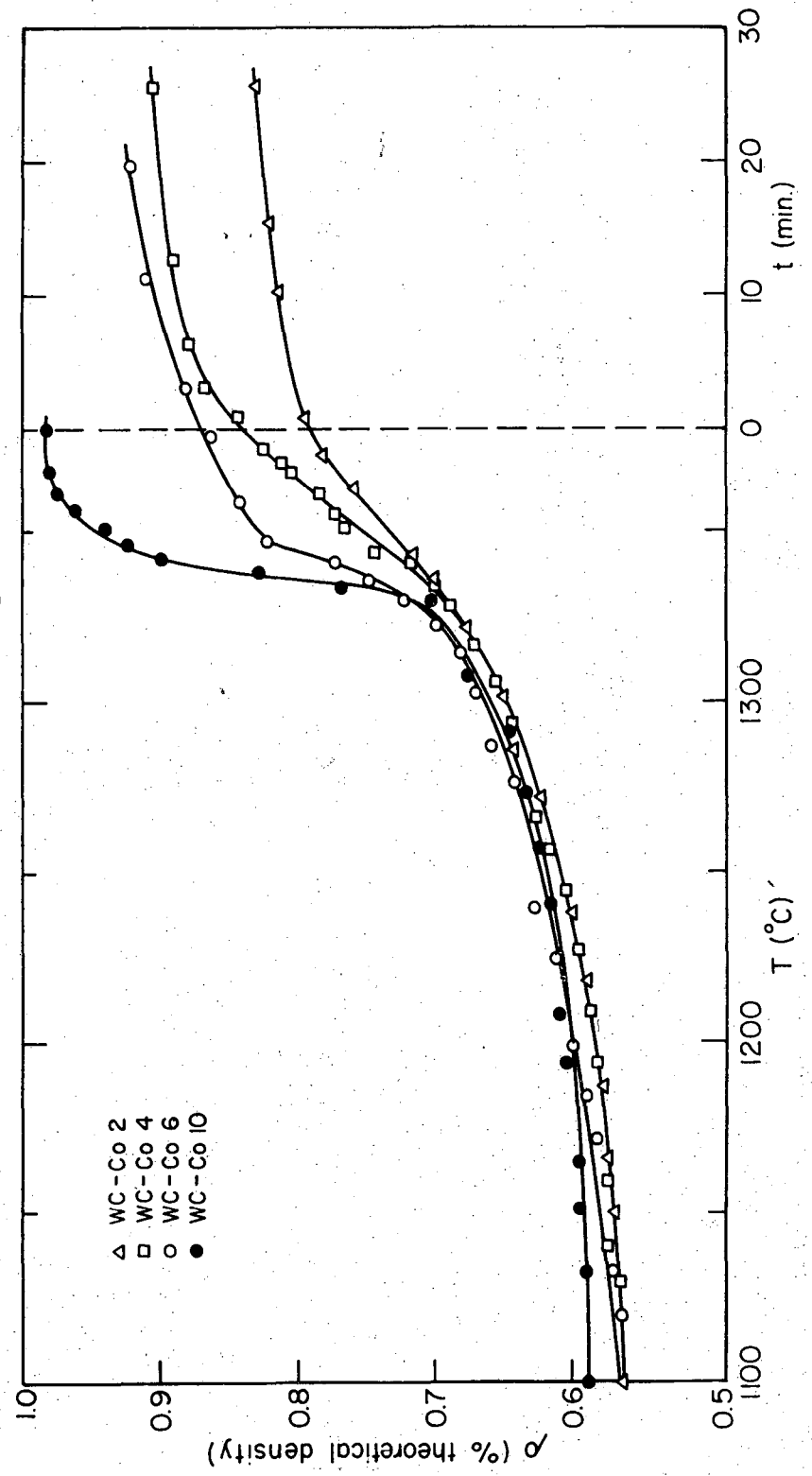

XBL 746-6584

Fig. 1

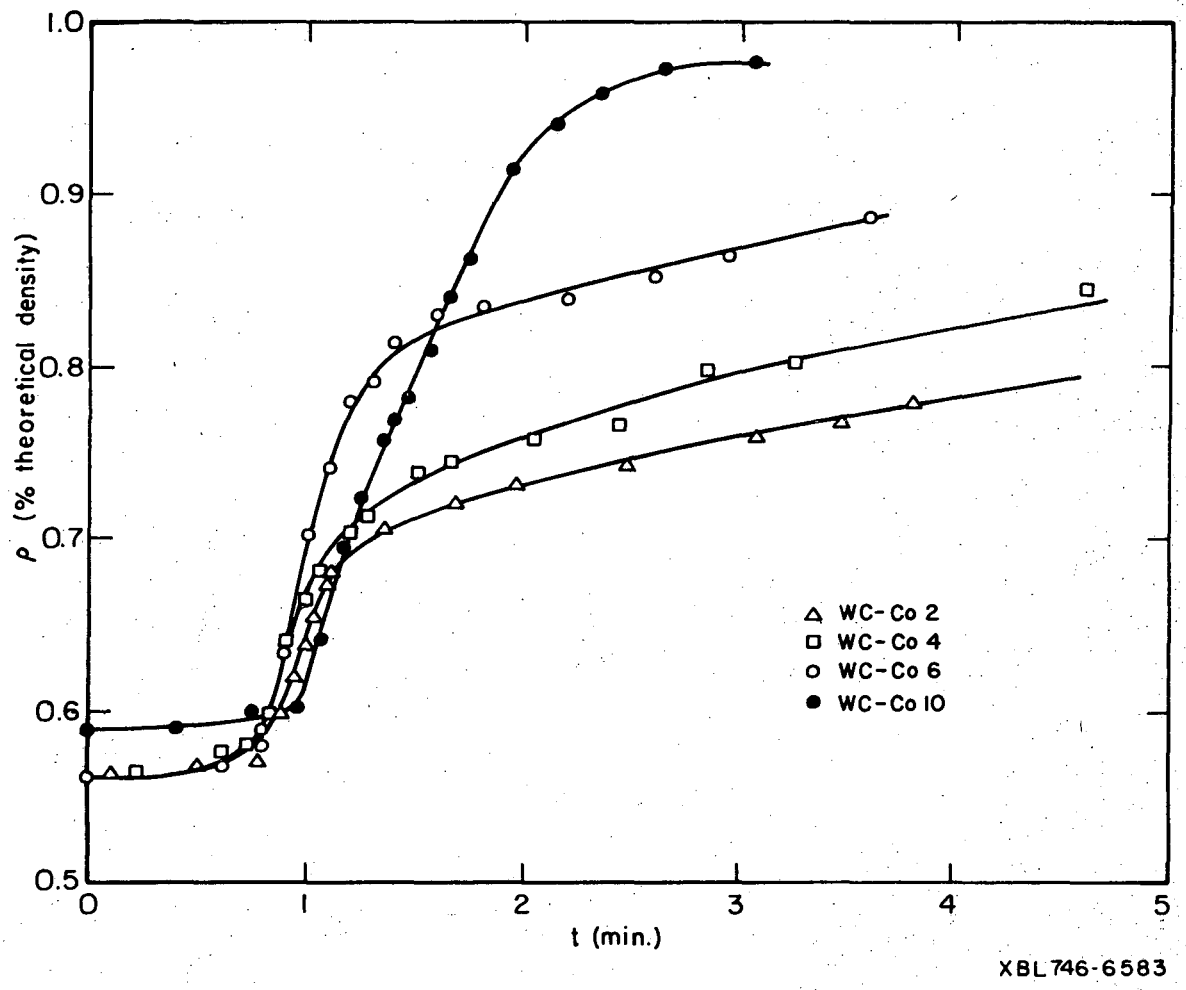
1.0
0.9
0.8
0.7
0.6
0.5
ρ (% theoretical density)
0
1
2
3
4
5
t (min.)
WC-Co 2
WC-Co 4
WC-Co 6
WC-Co 10
XBL 746-6583

Fig. 2

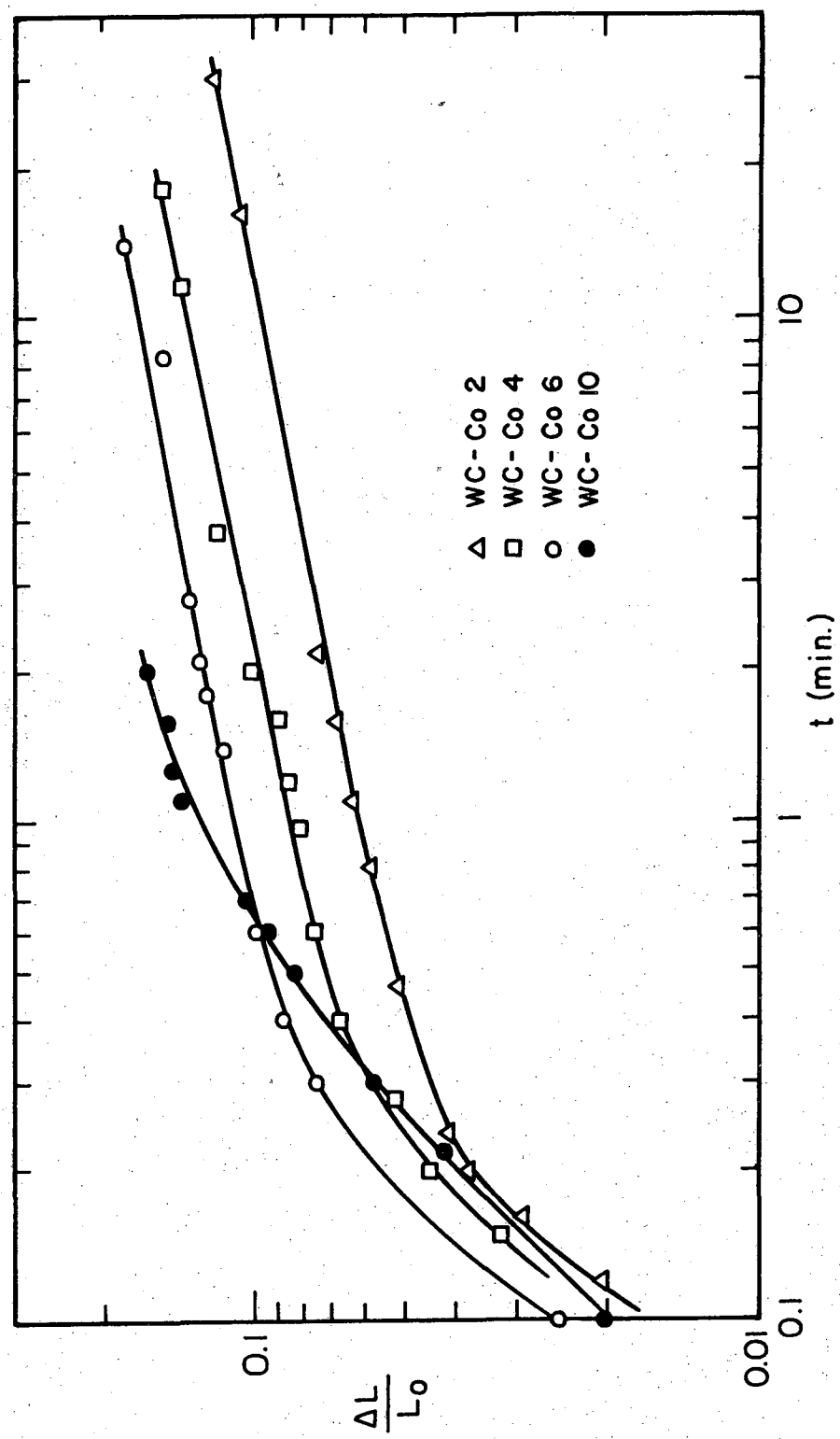

XBL 746-6582

Fig. 3

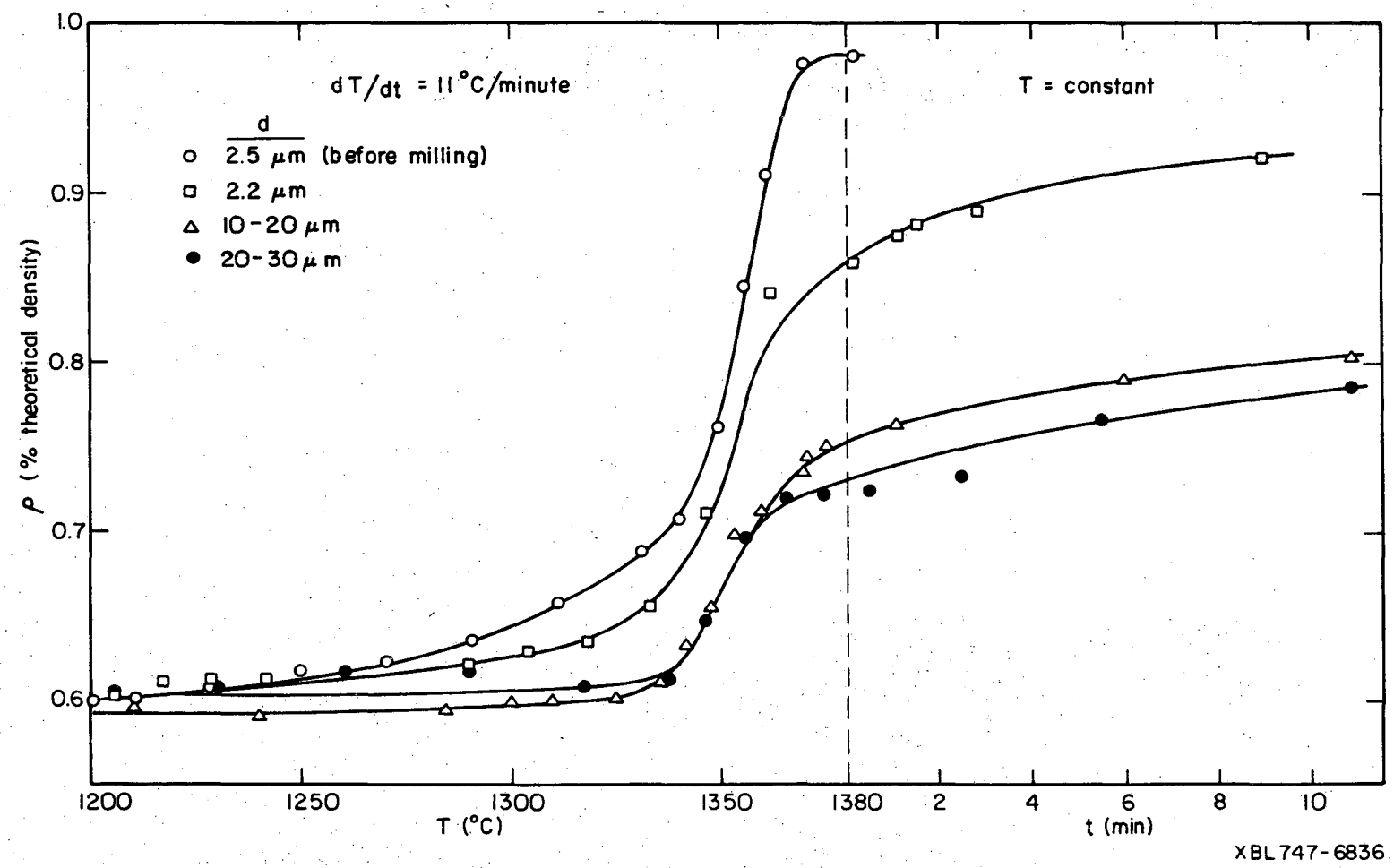
dT/dt = 11°C/minute
T = constant
d
2.5 μm (before milling)
2.2 μm
10-20 μm
20-30 μm
ρ (% theoretical density)
1.0
0.9
0.8
0.7
0.6
1200
1250
1300
1350
1380
2
4
6
8
10
T (°C)
t (min)
XBL 747-6836

Fig. 4

0 0 0 0 4 2 0 1 9 6 3

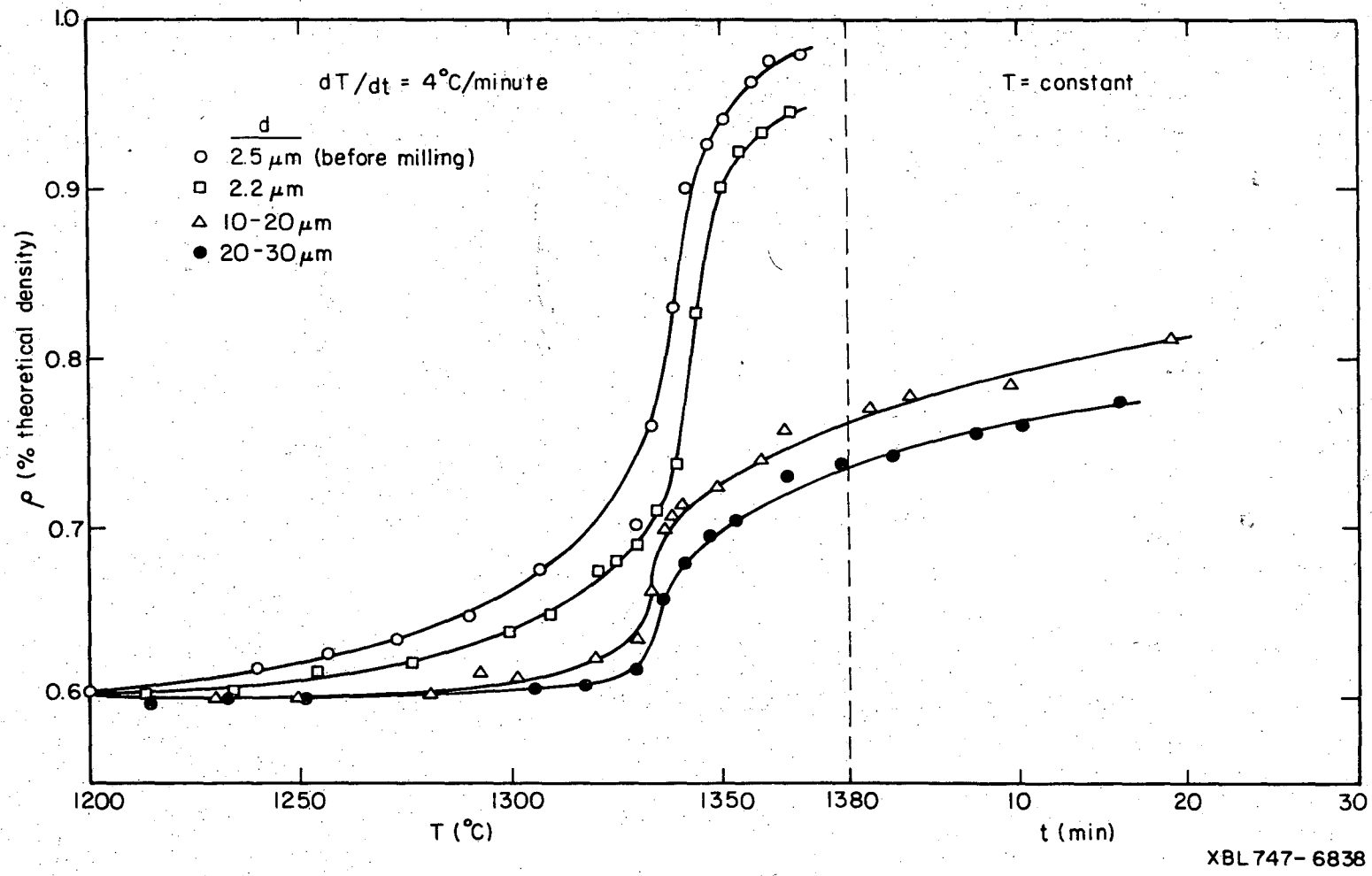

Fig. 5

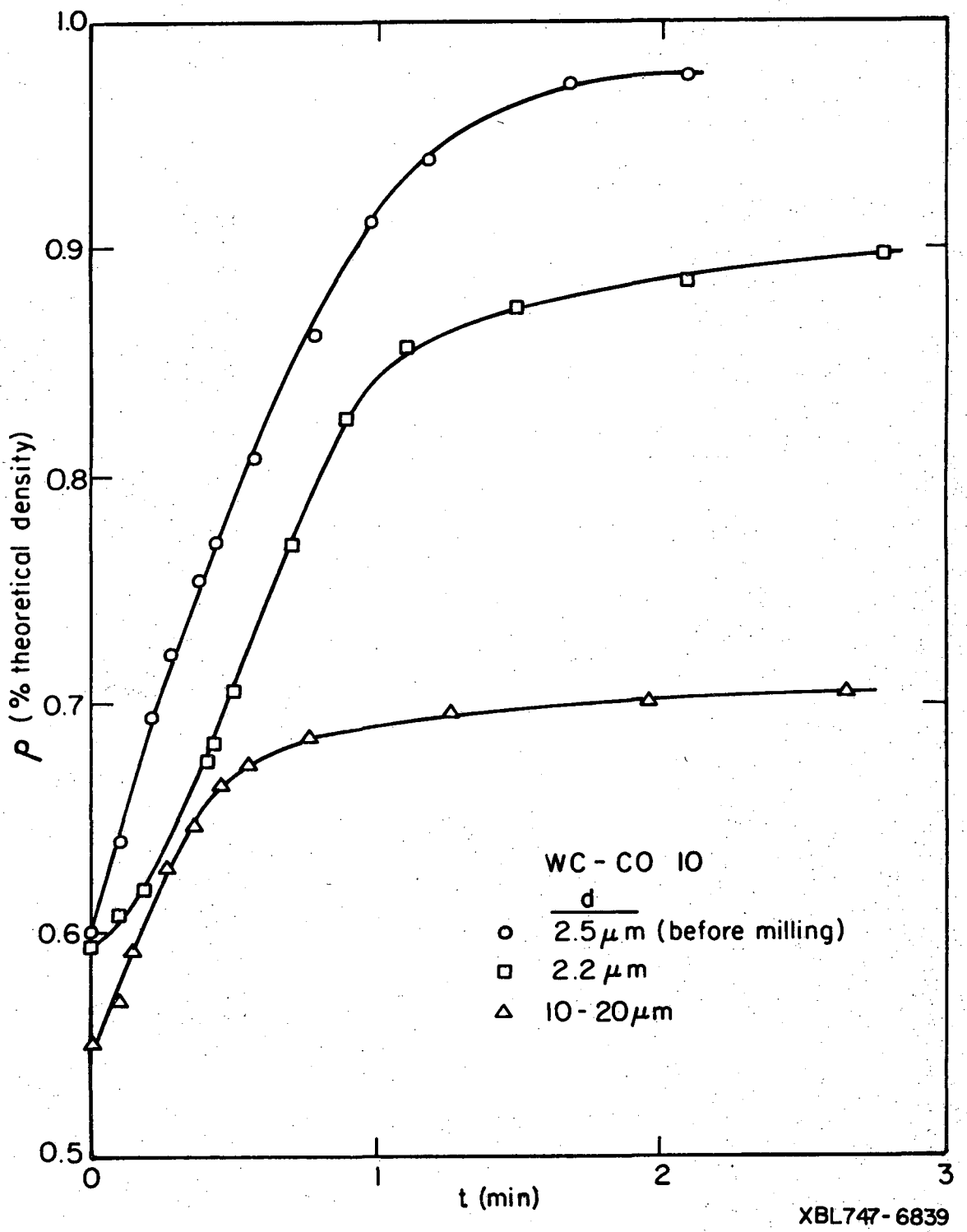
1.0
0.9
0.8
0.7
0.6
0.5
ρ (% theoretical density)
0
1
2
3
t (min)
WC - CO 10
d
2.5 μm (before milling)
2.2 μm
10 - 20 μm
XBL747-6839

Fig. 6

0 0 0 0 4 2 0 1 9 6 4

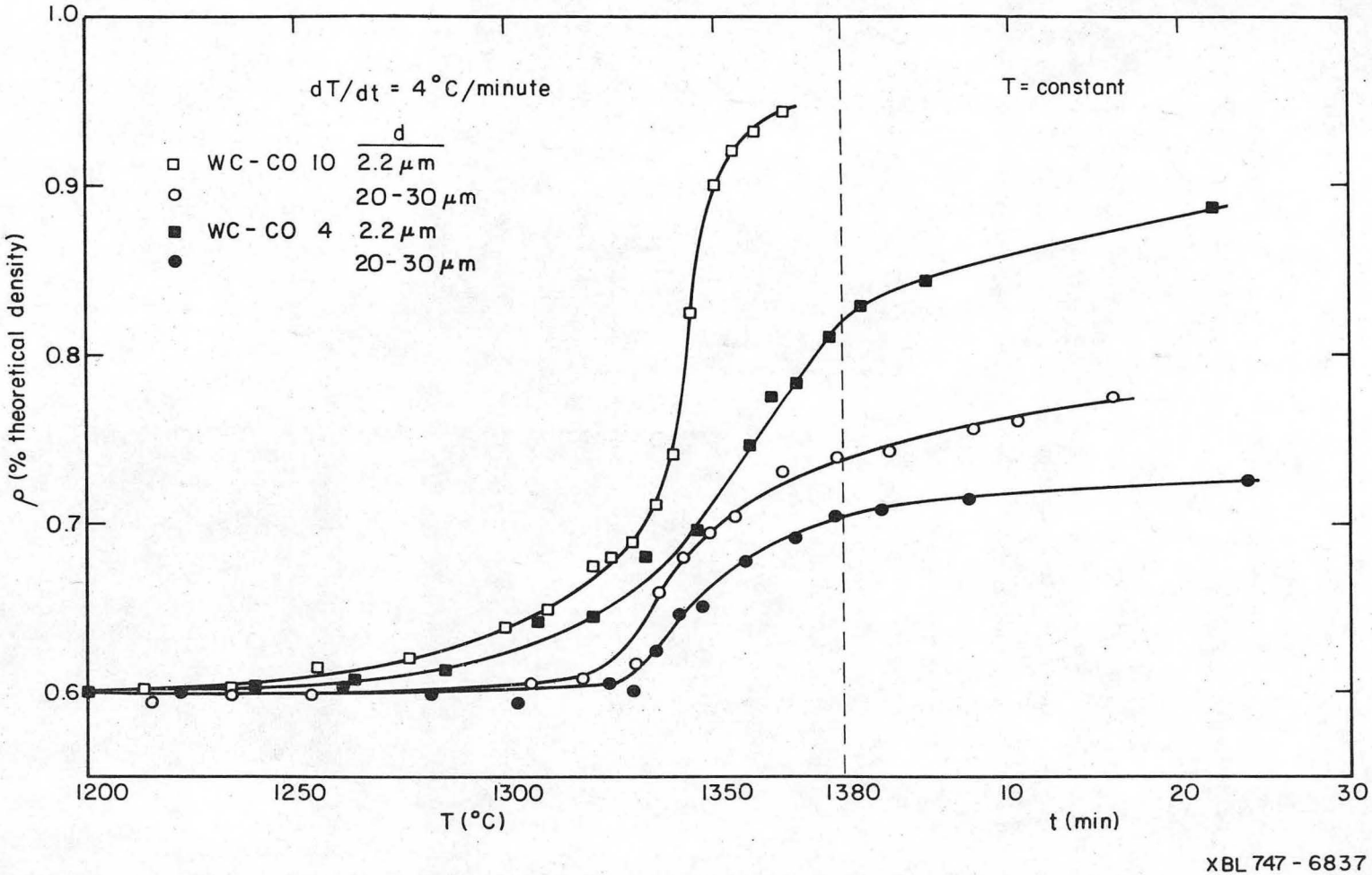

Fig. 7

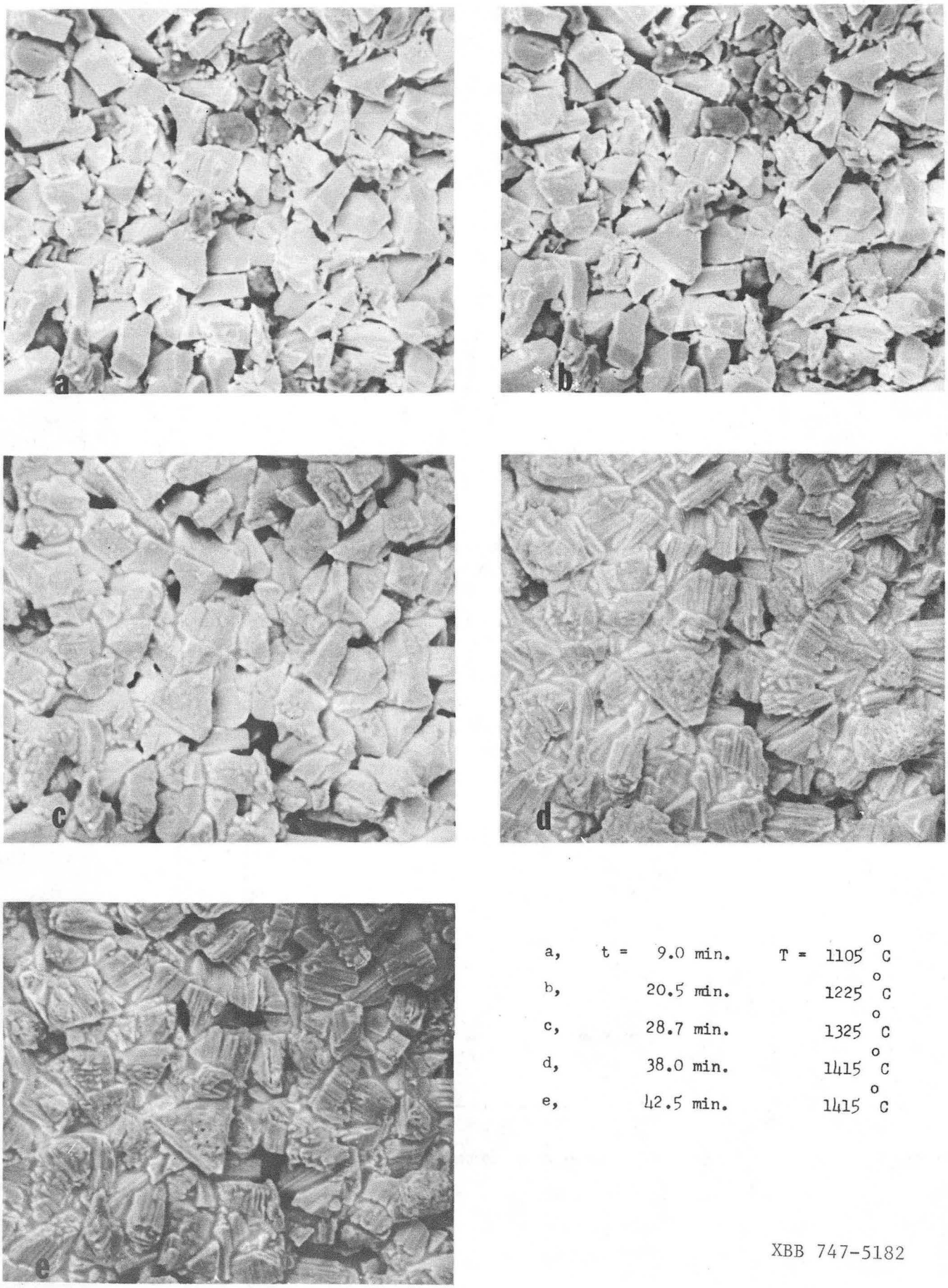

a,	t = 9.0 min.	T = 1105 °C
b,	20.5 min.	1225 °C
c,	28.7 min.	1325 °C
d,	38.0 min.	1415 °C
e,	42.5 min.	1415 °C

XBB 747-5182

Fig. 8

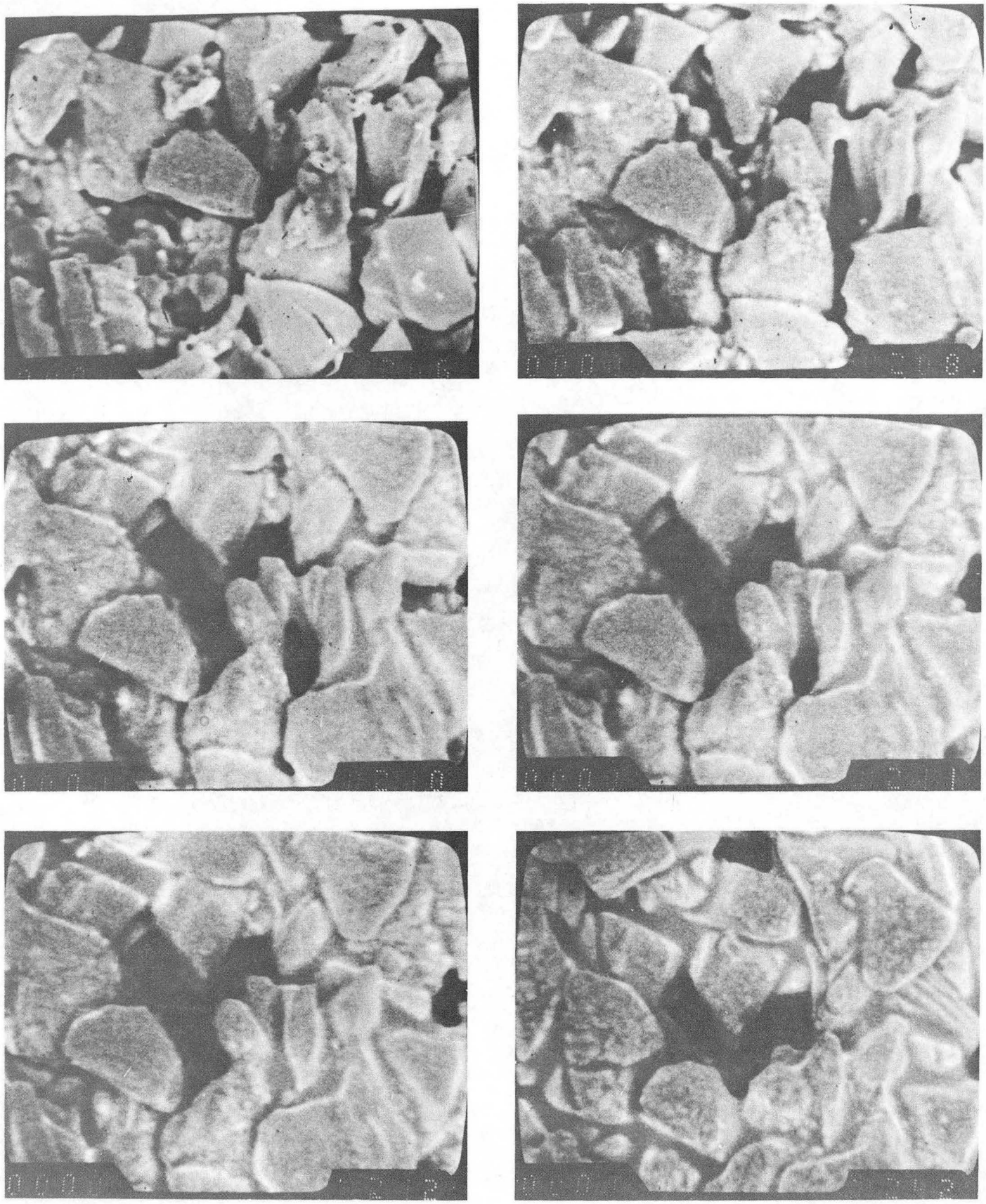

XBB 747-5181

Fig. 9

0 0 0 0 4 2 0 1 9 6 6

LEGAL NOTICE

This report was prepared as an account of work sponsored by the United States Government. Neither the United States nor the United States Atomic Energy Commission, nor any of their employees, nor any of their contractors, subcontractors, or their employees, makes any warranty, express or implied, or assumes any legal liability or responsibility for the accuracy, completeness or usefulness of any information, apparatus, product or process disclosed, or represents that its use would not infringe privately owned rights.

TECHNICAL INFORMATION DIVISION
LAWRENCE BERKELEY LABORATORY
UNIVERSITY OF CALIFORNIA
BERKELEY, CALIFORNIA 94720